Enhancement of *In Vivo* Anticancer Effects of Cisplatin by Incorporation Inside Single-Wall Carbon Nanohorns

Kumiko Ajima,[†] Tatsuya Murakami,[‡] Yoshikazu Mizoguchi,[‡] Kunihiro Tsuchida,[‡] Toshinari Ichihashi,[§] Sumio Iijima,[†,§,⊥,¶] and Masako Yudasaka[†,§,¶,*]

[†]SORST, Japan Science and Technology Agency c/o NEC, 34 Miyukigaoka, Tsukuba, Ibaraki 305-8501, Japan, [‡]Fujita Health University, Toyoake, Aichi 470-1192, Japan, [§]NEC 34 Miyukigaoka, Tsukuba, Ibaraki 305-8501, Japan, [⊥]Meijo University, 1-501 Shiogamaguchi, Tempaku-ku, Nagoya 468-8502, Japan, and [¶]AIST, Central 5, 1-1-1 Higashi, Tsukuba, 305-8565, Japan

ABSTRACT Cisplatin (CDDP) was incorporated inside single-wall carbon nanohorns with holes opened (SWNHox) by a nanoprecipitation method that involved dispersion of CDDP and SWNHox in a solvent followed by the solvent evaporation. The incorporated CDDP quantity increased from the previously reported value of 15 to 46%, and the total released quantity of CDDP also increased from 60 to 100% by changing the solvent from dimethylformamide to water. Concurrently, *in vitro* anticancer efficiency of CDDP@SWNHox increased to 4−6 times greater than that of the intact CDDP. *In vivo*, CDDP@SWNHox intratumorally injected to transplanted tumors of mice suppressed the tumor growth more than the intact CDDP. We observed that CDDP@SWNHox adhered to the cell surfaces *in vitro* and stayed within the tumor tissues *in vivo*. Therefore, we think that the CDDP released from SWNHox realized high concentrations locally at the cells *in vitro* and in the tissues *in vivo* and could efficiently attack the tumor cells. We also found that SWNHox itself had an *in vivo* anticancer effect, which might increase the anticancer activities of CDDP@SWNHox.

KEYWORDS: carbon nanohorn · cisplatin · drug delivery · anticancer activity · *in vivo*

Drug delivery systems (DDS) are designed to carry drugs selectively to the site of diseased tissues and to release the drugs slowly, thus minimizing the dose of drugs and reducing the drug side effects. To selectively reach the diseased sites, the DDS must be properly targeted, biocompatible, and nonstimulating toward the reticuloendothelial system. The constructions of DDS using liposomes,[1−3] polymer micelles,[4,5] and various other materials have been well investigated, some of which are successfully used in clinical levels. To cope with a wider variety of diseases, new carriers have been continuously sought. Recently, nanometer-sized materials have been highlighted as new types of DDS carriers. Among the nanomaterials, carbon nanotubes (CNTs)[6−8] and single-wall carbon nanohorns (SWNHs)[9−11] are unique for constructing the DDS because they are easily multifunctionalized. CNTs and SWNHs have plenty of inner spaces where the incorporation of the drugs is possible, and on the tube walls of CNTs and SWNHs, the drugs and various functional molecules can be physically adsorbed.[13] Further, the edges of the tube holes have oxidized functional groups where covalent attachment of chemicals are possible.[14,15] One of the unique DDS functions of the carbon nanotubules is the application of a plug on the holes, which would enable the precise control of the drug release. The plug function has been previously demonstrated using a SWNH with holes opened by oxidation (SWNHox): The Gd acetate was put at the holes as the plug, which controlled the release of C_{60} incorporated inside SWNHox.[16]

SWNHs have several advantages over CNTs. First, although the toxicity of CNTs appears to be low,[17] this aspect has not yet been clarified because toxicity tests are influenced by the contaminations with metal catalysts which are unavoidably used in the production processes.[18] Toxicological action of defects on the CNTs introduced by the purification processes for the removal of the metal catalysts[19] is unclear. On the other hand, no toxicity has been found for SWNH or SWNH in various animal tests.[20] Purity of SWNHs is high, 90−95%; they do not contain any metals, and they are useful as produced, with no need for further purification.[21,22] Second, the CNTs assemble to form bundles with micrometer-order length, while for the SWNH or SWNHox, thousands of them assemble to form a spherical aggregate with diameters of ~100 nm.[21] The 100 nm size meets the passive tumor-targeting condition of the enhanced permeability and retention. Materials with sizes of ~100 nm tend to accumulate at tumor tissues because of leakage of materials

*Address correspondence to m-yudasaka@aist.go.jp.

Received for review June 25, 2008 and accepted September 02, 2008.

Published online October 2, 2008.
10.1021/nn800395t CCC: $40.75

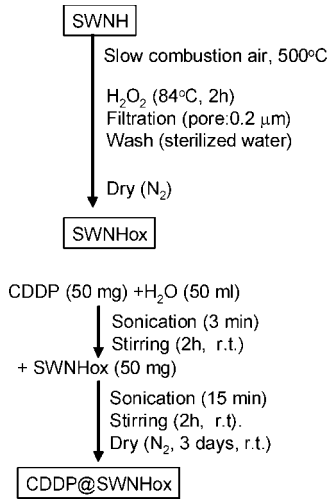

Figure 1. Preparation of cisplatin-incorporated single-wall carbon nanohorns with holes opened (CDDP@SWNHox).

out of the permeable tumor blood vessels and the poor lymphatic drainage.[4] Perhaps due to the 100 nm aggregate size SWNHox remain in the tumors for a longer time when injected intratumorally, leading to the improved inhibition effects on tumor growth caused by polyethylene glycol conjugated with doxorubicin (PEG-DXR) attached to the outside surface of SWNHox.[23] The third advantage of SWNHs comes from their large diameter and short length. CNTs have narrow diameters (1−2 nm) and long length (orders of micrometers), and the incorporation and release of drugs are not necessarily simple, and therefore, often the drugs are carried by attaching them to the outside walls.[6−8] In contrast, SWNHox have larger diameters (2−5 nm) and shorter length (40−50 nm),[21] and the incorporation of the drugs inside the SWNHox is easy. Furthermore, the drugs are released from the inside of SWNHox slowly.[9−12]

We have been investigating the application of DDS using SWNHs, and we show in this report that the quantities of cisplatin (*cis*-diaminedichloroplatinum(II), $Pt(NH_3)_2Cl_2$, CDDP),[10] an anticancer drug, incorporated inside SWNHox increase from 15[10] to 46% and are accompanied by increased release of CDDP in the medium. The results of *in vitro* and *in vivo* tests of CDDP incorporated into the SWNHox (CDDP@SWNHox) show

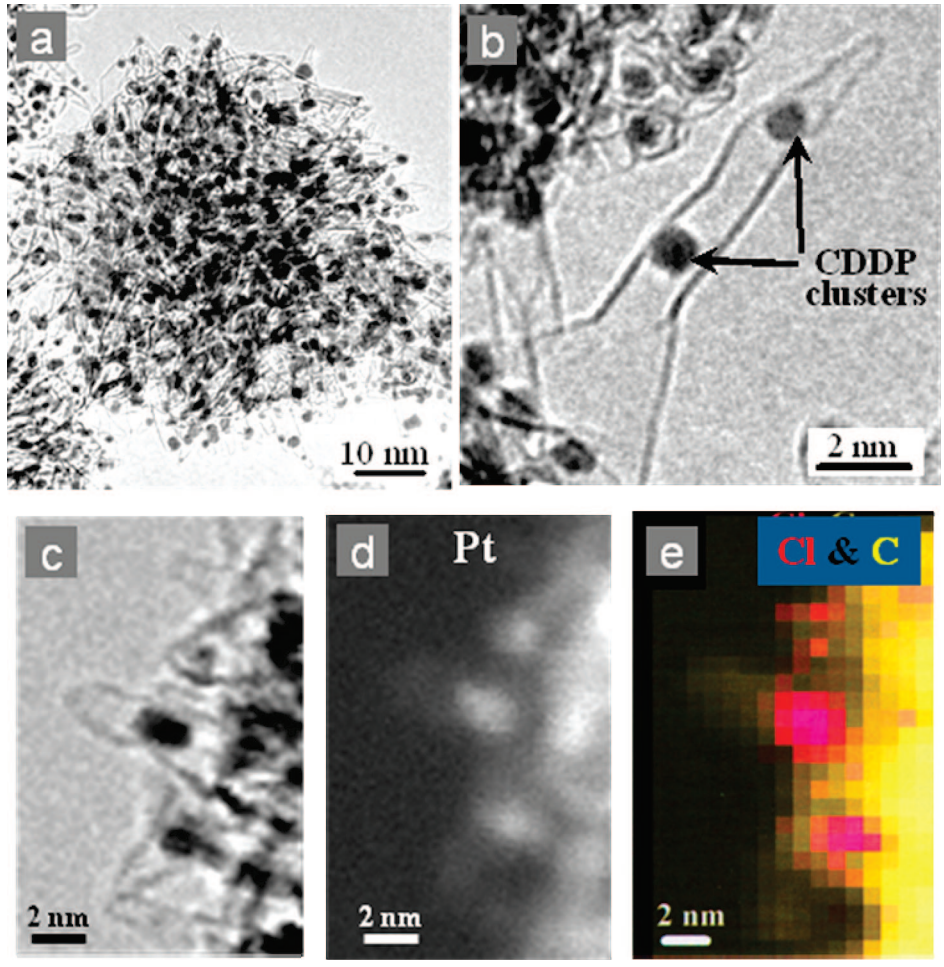

Figure 2. Transmission electron microscopy (a, b), scanning transmission electron microscopy (c), and *Z*-contrast (d) images of CDDP@SWNHox. Mapping of "C" and "Cl" was clarified by electron energy loss spectrum measurements (e). Observation or measurement for the images (c−e) were fixed at the same area. Black particles (a−c) are the CDDP clusters. Two CDDP clusters within one SWNHox sheath are indicated with arrows in (b). Bright spots in (d) correspond to Pt atoms in the CDDP clusters. Yellow and magenta areas in (e) indicate existences of C and Cl, respectively.

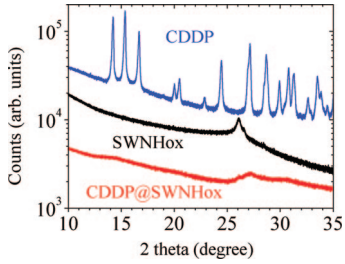

Figure 3. X-ray diffraction analysis of CDDP powder (blue line), SWNHox (black line), and CDDP@SWNHox (red line).

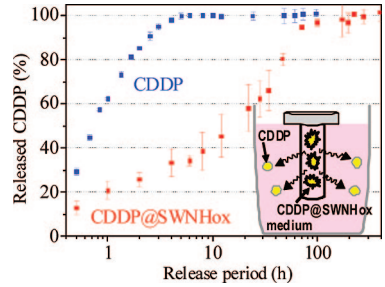

Figure 4. Release of CDDP from CDDP@SWNHox into a complete medium. The inset is a schematic illustration of the release quantity measurement system: CDDP alone (blue line) or CDDP@SWNHox (red line) (CDDP: 15 μM, 3 mL) in the dialysis membrane tube was dialyzed at room temperature for the indicated time. The quantities of the CDDP released into 600 mL of medium from CDDP@SWNHox were measured as described in the Materials and Methods.

the improvements in the anticancer effects. We have shown for the first time that SWNHox themselves have an *in vivo* antineoplastic effect, which might enhance the anticancer effect of CDDP@SWNHox *in vivo*.

RESULTS AND DISCUSSION

Structure of CDDP@SWNHox. CDDP@SWNHox were prepared by the nanoprecipitation method.[10,16] CDDP and SWNHox were dispersed in water, followed by the evaporation of the water (as outlined in Figure 1). Since water was used, the CDDP could have lost Cl atoms and changed to an aqueous complex.[24,25] Therefore, we examined the structure by transmission electron microscopy (TEM) and performed elemental analysis on CDDP@SWNHox. The TEM images of CDDP@SWNHox showed black spots of CDDP clusters over the size range of 1−5 nm incorporated inside SWNHox (Figure 2a,b). The CDDP clusters were also seen in the scanning transmission electron microscope (STEM) image as black spots (Figure 2c), and these clusters appeared as white spots in the *Z*-contrast image due to the Pt of CDDP (Figure 2d). In the *Z*-contrast image, atoms with large atomic numbers, such as Pt, appear as bright spots. An elemental mapping measured by electron energy loss spectrum (EELS) showed the locations of Cl (Figure 2e) almost coinciding with those of the CDDP clusters, suggesting that the CDDP structure was preserved. The number ratio of Pt and Cl atoms estimated from inductively coupled plasma optical emission spectroscopy (ICP) was about 1:2, which coincided with the 1:2 stoichiometry of Pt and Cl in CDDP, proving that the CDDP structure remained intact. The quantity of CDDP in CDDP@SWNHox estimated from the atomic absorption spectrum (AAS) was about 46%. We think that, even though the CDDP formed an aqueous complex when dissolved in water, the evaporation of water induced the back reaction, that is, the replacement of aqueous moieties by Cl, and the restoration of the aqueous complex to the CDDP molecule.

The CDDP quantity in the CDDP@SWNHox previously prepared by the same method but using DMF was about 15%. The formation of CDDP-DMF solvates[26] may hinder the incorporation of CDDP inside SWNHox, thereby limiting the CDDP incorporation quantity at about 15%.[10]

To confirm that no extra CDDP crystals contaminated the CDDP@SWNHox, X-ray diffraction (XRD) of CDDP@SWNHox was also measured (Figure 3). The result showed weak broad peaks appearing at about 14, 27, and 31° but no sharp diffraction peaks characteristic of the intact CDDP (Figure 3). The weak broad peaks probably arose from the small-sized CDDP clusters located inside SWNHox, as seen in the microscopic images of CDDP@SWNHox (Figure 2). The peak at ~26° represented the diffraction from graphitic particles which were contained in the initial SWNH at a concentration of about 10%.[22,27]

Release of CDDP from CDDP@SWNHox. The release of CDDP from CDDP@SWNHox was evaluated by using dialysis cellulose tubes immersed in the complete culture me-

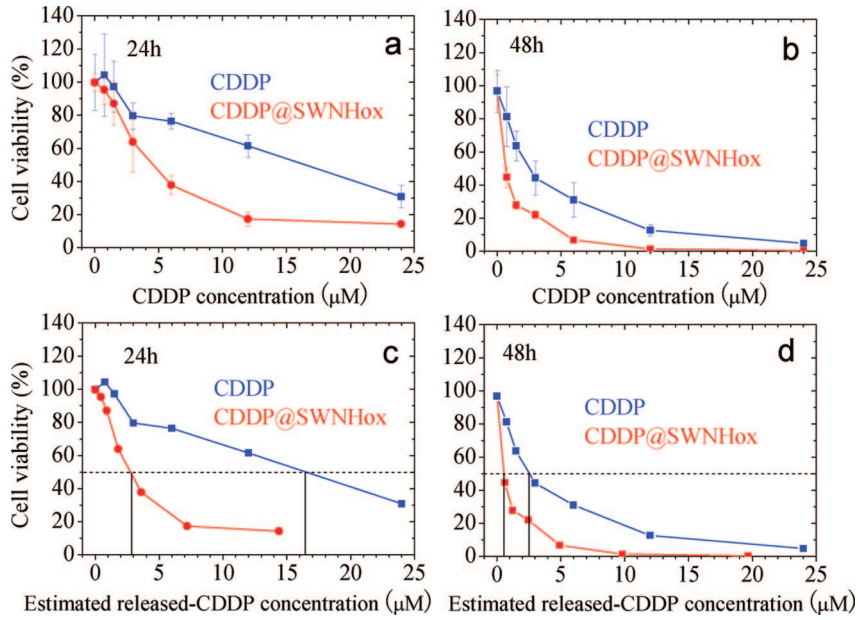

Figure 5. Cell (H460) viability depending on the dose quantity of CDDP (blue lines) and CDDP@SWNHox (red lines). Incubation periods were 24 h (a, c) and 48 h (b, d).

dium. The intact CDDP was dissolved in the complete medium and was put in the dialysis tube. Almost 100% of the CDDP diffused from the cellulose tube in 5 h (Figure 4). However, CDDP@SWNHox examined similarly showed much slower profiles, taking ~150 h for the 100% release. We inferred that the release of CDDP from inside the SWNHox was slower because the CDDP clusters gained a certain stabilization energy by the confinement inside the narrow nanometer-scale spaces.

When CDDP@SWNHox was prepared using DMF,[10] the CDDP release saturated at lower levels, about 60%, which could be again due to the formation of CDDP-DMF solvates,[26] some of which are probably highly stabilized inside the SWNHox.

***In Vitro* Anticancer Activities.** Although CDDP was slowly released from CDDP@SWNHox (Figure 4), it exhibited higher efficiency for killing human lung cancer cells, NCI-H460, than did the intact CDDP (Figure 5a,b). This effect is more clearly shown if the data are expressed in terms of the released CDDP quantities that were estimated from Figure 4 as (CDDP dosed-quantity in Figure 5a,b) × (released percent at 24 or 48 h in Figure 4)/100. After incubation for 24 h (Figure 5c), the amount of CDDP derived from CDDP@SWNHox at the 50% viability level was about 1/6 of that when the intact CDDP was administered. Likewise, after 48 h incubation (Figure 5d), the quantity of CDDP released from CDDP@SWNHox that afforded 50% cell death was about 1/4 of the concentration required to achieve the same level of cell death for free CDDP. It should be noted that the SWNHox alone did not show any *in vitro* cytotoxicity, as we previously reported.[9−12]

To examine how the smaller quantities of CDDP of CDDP@SWNHox could efficiently kill the cancer cells, sections of cells were observed with optical microscopy. Comparing the images of cells incubated for 5 h without any addition of the specimens (Figure 6a,b) and those of the cells incubated with SWNHox (Figure 6c,d) or with CDDP@SWNHox (Figure 6e,f), it is clear that black particles of SWNHox or CDDP@SWNHox attached to the cells. The black particles were agglomerates of spherical aggregates of SWNHox or CDDP@SWNHox, which were found by observations at a higher magnification using STEM (Figures 6g−i).

Due to the proximity of the CDDP@SWNHox near the cancer cells, diffusion was minimized and the drug concentration near the cells remained high, and the high concentration was maintained for a considerably longer time due to the attenuated release of the CDDP. This effect may explain the greater antineoplastic effects found in the cell assays (Figure 5).

***In vivo* Anticancer Effects.** We used nude female mice (BALB/c *nu/nu*) on which the tumors were subcutaneously transplanted on day 0. The specimens (saline, CDDP, SWNHox, CDDP@SWNHox) were intratumorally injected twice, on day 11 and day 15. The variations in

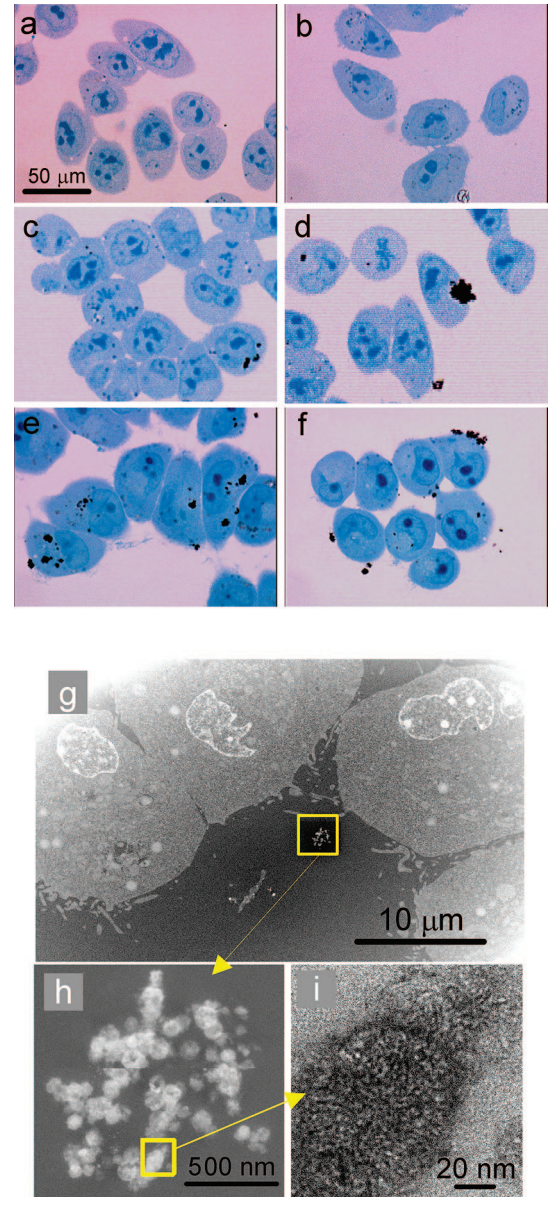

Figure 6. Optical microscopy images of sections of N460 cells incubated for 5 h without addition (a, b) and with additions of SWNHox (c, d) and CDDP@SWNHox (e, f). *Z*-contrast images of the cell sections incubated with CDDP@SWNHox for 5 h (g−i).

tumor sizes and body weights were documented (Figure 7). Compared to the saline injection (Figure 7a), the SWNHox injection (0.5 mg/kg) appreciably suppressed the tumor growth (Figure 7b), indicating that SWNHox itself had certain anticancer effects, which we show here for the first time, although it is not as effective as CDDP (0.5 mg/kg) (Figure 7c). CDDP@SWNHox (CDDP 0.5 mg/kg, SWNHox 0.5 mg/kg) showed higher anticancer effect (Figure 7d) than the intact CDDP, indicating the enhancement of CDDP efficiency by the incorporation inside SWNHox.

The body-weight decrease can be a measure of negative side effects. The measured body-weight decreases were within 10% when the control and

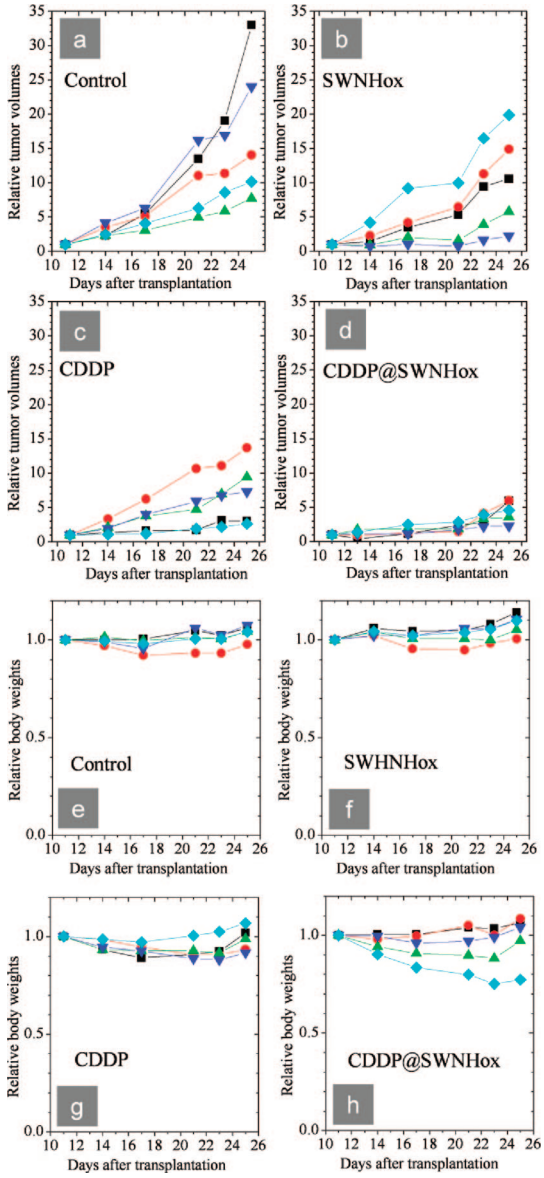

Figure 7. Relative tumor volumes and weights normalized at unity on day 11. Saline (a, e), SWNHox (b, f), CDDP (c, g), and CDDP@SWNHox (d, h) were intratumorally injected on day 11. The dosages of CDDP were 0.5 mg/kg. In each graph, the results of five mice are shown. The tumor size and weight of a mouse are shown with the same color.

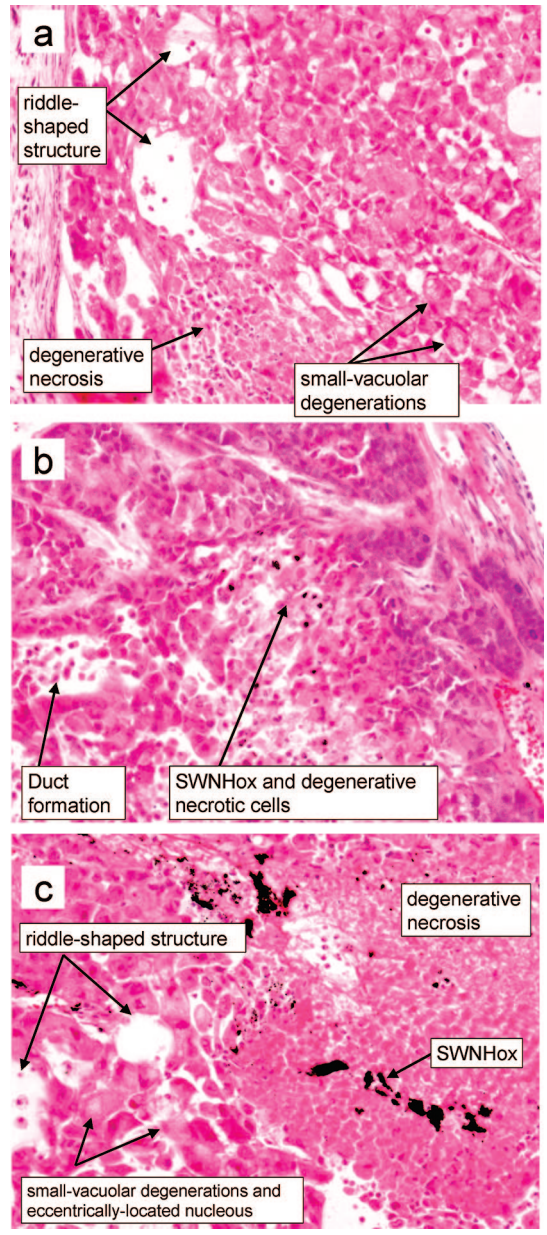

Figure 8. Optical microscopic images of tumor tissue sections. CDDP (a), SWNHox (b), and CDDP@SWNHox (c) were intratumorally injected on day 11, and the tumors were excised on day 25.

SWNHox were injected (Figure 7e,f), while the weight decreases were a little larger when CDDP and CDDP@SWNHox were injected (Figure 7g,h), suggesting that adverse effects of CDDP were a little expressed. The body-weight decrease of one mouse treated with CDDP@SWNHox (Figure 7h, pale blue curve) was appreciably larger than those of the other mice, for which the reason was not clear in our test this time. Since the body weight started to increase in the latter part of the test periods (Figures 7g,h) in all cases, we consider that the negative side effects caused by using SWNHox, as reflected by the weight decrease, were not critical.

Observation of Tumor Tissue Sections. To determine why the antitumor effect of CDDP@SWNHox was stronger than that of CDDP, and why SWNHox could have an antitumor effect, we anatomized the mice on day 25, made the tumor tissue sections, and observed them with an optical microscope. The degeneration caused by the intact CDDP was remarkable: small vacuolar degenerations in cytoplasm and eccentric nuclei were apparent, which would lead to the necrosis (Figure 8a). CDDP@SWNHox induced small vacuolar degenerations, eccentric nuclei, and necrosis around the places where the CDDP@SWNHox agglomerates existed (Figure 8c). Interestingly, the SWNHox administration induced the

vacuolar-like degeneration, suggesting that SWNHox alone were toxic to the tumor tissues (Figure 8b).

The observation of the sections revealed that SWNHox and CDDP@SWNHox stayed in the tumor tissues even at 25 days after the administration. This tendency was also see in a previous report in which PEG-DXR/SWNHox intratumorally injected into subcutaneously transplanted tumors (day 0) remained in the tumor tissues even on day 21.[23]

These results indicate that CDDP@SWNHox can efficiently supply CDDP to the tumor tissues by staying in the tumors. Although the CDDP was slowly released from CDDP@SWNHox, the incorporated CDDP quantity was abundant, and therefore, the quantity of slowly released CDDP was sufficient to kill the tumor cells. The weaker antitumor effect of the intact CDDP might be caused by its dissipation outside the tumor sites into the blood, body fluid, and/or lymph.

From the tissue section observations, we confirmed the antitumor effect of SWNHox, suggesting that SWNHox might enhance the anticancer efficiency of CDDP@SWNHox. However, it is impossible to infer why the SWNHox had such effect. More investigations are necessary to clarify this issue. We propose that the antitumor effect of SWNHox might be specific to the tumor sites because we did not find any toxicity of SWNHox *in vivo* using normal mice[20] and also *in vitro*.[9−12]

SUMMARY

By changing the solvent used in the incorporation process from the previous DMF to water, we achieved an increase in the quantity of CDDP incorporated into SWNHox from the previous 15% up to 46%. The slow release of CDDP from CDDP@SWNHox was comparable with previous studies, but the total released quantity increased from previous 60 to 100%. The disadvantage of using DMF could be originated from the formation of CDDP-DMF solvates.

The CDDP@SWNHox had a higher antitumor efficiency than the intact CDDP, which was confirmed *in vitro* and *in vivo*. We believe that the enhancement of anticancer efficiency *in vitro* was caused by the adherence of SWNHox to the cells, which would increase the local (=near-cell) concentration of CDDP released from CDDP@SWNHox, leading to effective cell killing. Since the quantity of CDDP of CDDP@SWNHox was large (46%) and total released quantity was high (100%), the slowly released CDDP could maintain this high local concentration over a long period.

In vivo, the CDDP@SWNHox stayed in the tumor tissues for a considerable period, up to 25 days, which contributed to the higher anticancer efficiency of CDDP@SWNHox as compared to the intact CDDP. The *in vivo* anticancer effect of SWNHox itself was found for the first time in this study, although no toxicity of SWNH or SWNHox has been found in the normal tissues in normal animal tests done independently from this study.

MATERIALS AND METHODS

Sample Preparation and Analysis. SWNHs were prepared by the CO_2 laser ablation of graphite without any metal catalysts in Ar gas (760 Torr) at room temperature.[21,22] To open the holes, SWNHs were oxidized by the slow combustion method[28] wherein the temperature was elevated from room temperature to 500 °C at a rate of 1 °C/min in dry air, followed by natural cooling. To increase the number of −COOH groups at the hole edges, the SWNHs were further oxidized with aqueous solution of H_2O_2 (~30%) at 84 °C for 2 h, followed by washing with sterilized water and drying under N_2 flow (see Figure 1).

CDDP was incorporated inside SWNHox by the nanoprecipitation method:[10,16] 50 mg of CDDP was dissolved in 50 mL of sterilized water in a beaker by sonication for 3 min and stirring for 2 h at room temperature. Into this solution, 50 mg of SWNHox was mixed, sonicated for 15 min, and stirred for 2 h at room temperature. The obtained dispersion was placed in flowing nitrogen gas at room temperature for about 3 days in the dark until the solvent was evaporated. Black powders of CDDP@SWNHox were obtained at the bottom of the beaker. The excess CDDP was deposited as yellow CDDP crystals on the side walls of the beaker, which were easily discriminated from the CDDP@SWNHox black powder.

The structure of CDDP@SWNHox was observed with high-resolution TEM (002B, Topcon, 120 kV) and STEM with *Z*-contrast imaging (HD-2300, Hitachi, 120 kV). Mapping of chlorine (Cl) of CDDP was measured with EELS. XRD was measured to confirm that there was no crystallized CDDP contaminating the CDDP@SWNHox.

The quantity of CDDP ($Pt(NH_3)_2Cl_2$) in CDDP@SWNHox was calculated from the Pt quantity estimated from AAS (Z-2700, Hitachi). For the AAS measurements, CDDP@SWNHox dispersions were prepared as follows: CDDP@SWNHox was mixed with a 0.1% aqueous solution of a surfactant, TWEEN20 at a concentration of 0.1 mg/mL, and treated with a homogenizer (UP 400s, Ultraschall processor, Dr. Hielscher Gmbh) at 240 W with a cycle of 0.5 s^{-1} for 15 min. The dispersion thus homogenized was diluted 1/100 with an aqueous 5% HCl solution, and the AAS was measured at 265.9 nm. The calibration curve of Pt concentration against the AAS intensity was performed by using Pt 1000 Platinum Standard Solution (Pt 1006 mg/L) diluted to less than 300 ppb with 5% aqueous HCl.

The number ratios of Pt and Cl were estimated from ICP (ULTIMA2, HORIBA) measurements. For these measurements, CDDP@SWNHox were dispersed in 0.1% TWEEN 20 aqueous solution at a concentration of 0.1 mg/mL and sonicated for 15 min. The Pt emission line used was at 265.945 nm. In the case of the Cl emission line, the second diffracted line of 67.362 nm, 134.724 nm, was detected. The intensity concentration calibration was done using a solution of CDDP (0−0.05 mg/mL) dissolved in 0.1% aqueous solution of TWEEN 20.

Release Rate Measurements. The CDDP@SWNHox were dispersed in 3 mL of a culture medium, RPMI 1640, wherein the CDDP quantity was set at 4.6 μg mL^{-1} (=15 μM). The control was the intact CDDP dissolved in the medium (15 μM). The intact CDDP or CDDP@SWNHox dissolved in the medium were placed in the dialysis membrane cellulose tube (Float-A-Lyzer, Biotech CE, Spectrum Laboratories Inc.; pore diameter of about 4 nm and molecular weight cutoff of about 100 kDa). The dialysis units were immersed in 600 mL of the medium. The CDDP released from SWNHox diffused from the cellulose tube, but the SWNHox nanostructures did not. The CDDP solution outside of the cellulose tube was diluted 1/6 with 5% HCl aqueous solution, and the Pt quantity was measured with AAS.

Cell Preparation. Immunodeficient 4 week old athymic nude female mice (BALB/c *nu/nu*) were purchased from CLEA (CLEA Ja-

pan Inc., Tokyo, Japan) and housed in a specific pathogen-free animal facility at Fujita Health University in accordance with the regulations of the University's committee on the Use and Care of Animals. Animals were fed *ad libitum* with γ-irradiated rodent diet CE2 (CLEA Japan Inc.).

Nonsmall human lung cancer cells, NCI-H460, were purchased from the National Cancer Institute (Frederick, MD) and were maintained in the complete culture medium (RPMI 1640 supplemented with 10% fetal bovine serum and penicillin streptomycin). These cells were incubated at 37 °C under a humidified atmosphere of 5% CO_2 and 95% air and were passaged every 3−4 days. The NCI-H460 cells were harvested with 0.25% trypsin−EDTA solution, washed, and resuspended in a 1:1 mixture of RPM I1640 and Matrigel. The cell suspension (1.0×10^6 cells in 50 μL) was administered subcutaneously into the left flank of a mouse using a 26 gauge needle. The tumors were allowed to grow for 1 week until reaching ~100 mm^3. The tumors were then excised and homogenized in phosphate buffered saline (PBS) with a mixer. The obtained mixture was centrifuged, and the sediments were taken out. The sediments containing the NCI-H460 cells were seeded in the complete medium. After several time passages, the NCI-H460 cells were subcutaneously injected, thus the *in vivo* passage was applied twice. After the second passage, we used the extracted NCI-H460 for *in vitro* and *in vivo* tests of the intact CDDP, SWNHox, and CDDP@SWNHox.

***In Vitro* Anticancer Activity.** The cytotoxicity of CDDP released from the CDDP@SWNHox against NCI-H460 was evaluated with an assay using WST-1 (4-[3-(4-iodophenyl)-2-(4-nitrophenyl)-2*H*-5-tetrazolio]-1,3-benzene disulfonate) (Roche Diagnostics). This colorimetric assay quantifies cell proliferation and cell viability and is based on the reduction of the WST-1 into formazan by mitochondrial dehydrogenases in living cells. The cells were seeded in the complete medium. Aliquots (100 μL) of cell suspension with a cell concentration of 5×10^4 mL^{-1} were placed in each well of 96-well microplates and were cultivated at 37 °C in humidified air with 5% CO_2 for 6 h to permit cell adhesion to the cell dishes. The CDDP and CDDP@SWNHox were dispersed in the culture medium with various CDDP concentrations (0−24 μM). After removal of the culture medium from the cell-culturing microplate dishes, 100 μL of the dispersion of CDDP or CDDP@SWNHox was added to each cell dish, followed by the incubation at 37 °C in 5% CO_2 for 48 h. After the 48 h incubation, CDDP or CDDP@SWNHox was removed from each well, and 110 μL of the WST-1 diluted with the culture medium (10 μL WST-1/100 μL culture medium) was dropped into the well. After incubation for 1 h, the cell viabilities were monitored by measuring the light absorbance at 450 nm using a microplate reader (680 microplate reader, Bio-Rad). The base absorbance was taken at 595 nm.

Preparation of Cell Sections for Microscopic Observation. NCI-H460 cells were incubated in the complete medium containing CDDP, SWNHox, or CDDP@SWNHox for 5 h, then washed with PBS several times. The washed cells were immersed in 2% formalin and fixed by 2% glutaraldehyde solution, followed by immersing in 0.1 M phosphate buffer for one night at 4 °C, 1% osmium tetraoxide fixing solution, 70 and 100% ethanol solution each for 30 min, propylene oxide for 1 h twice, and Epon embedding for 3 days at 60 °C. The Epon-embedded blocks were sliced at 1 μm and stained with methylene blue for the optical microscopic observation (Axioplan, Zeiss). For the electron microscopic observation STEM (HD2300, Hitachi), the cells were sliced (LKB U5 Ultramicrotome, Amersham Pharmacia) at 80−100 nm followed by staining with uranyl acetate for 10 min and Reynolds lead for 3 min.

***In Vivo* Anticancer Activity.** According to the same protocol introduced in the section Cell Preparation, NCI-H460 was subcutaneously transplanted in the mice (BALB/c *nu/nu*) (day 0). On days 11 and 15, the mice were treated intratumorally with saline (9% aqueous solution of NaCl, Otsuka), SWNHox, CDDP, or CDDP@SWNHox dispersed in the medium. The administered dose of the saline was 5 mL/kg, and that of CDDP was 0.5 mg/kg. The size of the tumor was measured along the longest width (*W*) and the corresponding perpendicular length (*L*). The formula chosen to compute tumor volume (*V*) was for a standard volume of an ellipsoid, where $V = 4\pi/3$ (length/2 × width/2 × depth/2). Assuming that depth equals width and π equals 3, $V = 1/2 \times L \times W^2$. The relative tumor volume was calculated as (volume of the tumor on the day of measurement)/(volume of the tumor on the day 11).

Preparation of Tumor Tissue Sections for Microscopic Observation. The excised tissues near the center of tumors (day 25) were fixed in 4% paraformaldehyde overnight. The tissues were then processed for paraffin embedding. Multiple 3 μm thick microtome sections from each tissue were dewaxed, hydrated, and stained with hematoxylin and eosin by standard method.

Acknowledgment. We thank Takeshi Azami and Daisuke Kasuya (NEC Co.) for preparing the SWNHs, and Keisuke Hitachi for picture drawings.

REFERENCES AND NOTES

1. Yatvin, M. B.; Weinstein, J. N.; Dennis, W. H.; Blumenthal, R. Design of Liposomes for Enhanced Local Release of Drugs by Hyperthermia. *Science* **1978**, *202*, 1290–1293.
2. Allen, T. M. Liposomal Drug Formulations. *Drugs* **1998**, *56*, 747–756.
3. Burger, K. N. J.; Staffhorst, R. W. H. M.; de Vijlder, H. C.; Velinova, M. J.; Bomans, P. H.; Frederik, P. M.; de Kruijff, B. Nanocapsules: Lipid-Coated Aggregates of Cisplatin with High Cytotoxicity. *Nat. Med.* **2002**, *8*, 81–84.
4. Yokoyama, M.; Miyauchi, M.; Yamada, N.; Okano, T.; Sakurai, Y.; Kataoka, K.; Inoue, S. Characterization and Anticancer Activity of the Micelle-Forming Polymeric Anticancer Drug Adriamy-cinconjugated Poly(ethylene glycol)-Poly(aspartic acid) Block Copolymer. *Cancer Res.* **1990**, *50*, 1693–1700.
5. Nishiyama, N.; Okazaki, S.; Cabral, H.; Miyamoto, M.; Kato, Y.; Sugiyama, Y.; Nishio, K.; Matsumura, Y.; Kataoka, K. Novel. Cisplatin-Incorporated Polymeric Micelles Can Eradicate Solid Tumors in Mice. *Cancer Res.* **2003**, *63*, 8977–8983.
6. Pantarotto, D.; Briand, J.-P.; Prato, M.; Bianco, A. Translocation of Bioactive Peptides Across Cell Membranes by Carbon Nanotubes. *Chem. Commun.* **2004**, *1*, 16–17.
7. Singh, R.; Pantarotto, D.; McCarthy, D; Chaloin, O.; Hoebeke, L.; Partios, C. D.; Briand, J.-P.; Prato, M.; Bianco, A.; Kostarelos, K. Binding and Condensation of Plasmid DNA onto Functionalized Carbon Nanotubes: Toward the Construction of Nanotube-Based Gene Delivery Vectors. *J. Am. Chem. Soc.* **2005**, *127*, 4388–4396.
8. Kam, N. W. S.; Liu, Z.; Dai, H. Functionalized Carbon Nanotubes *via* Cleavable Disulfide Bonds for Efficient Intracellular Delivary of siRNA and Potent Gene Silencing. *J. Am. Chem. Soc.* **2005**, *127*, 12492–12493.
9. Murakami, T.; Ajima, K.; Miyawaki, J.; Yudasaka, M.; Iijima, S.; Shiba, K. Drug-Loaded Carbon Nanohorns: Adsorption and Release of Dexamethasone *In Vitro*. *Mol. Pharm.* **2004**, *1*, 399–405.
10. Ajima, K.; Yudasaka, M.; Murakami, T.; Maigné, A.; Shiba, K.; Iijima, S. Carbon Nanohorns as Anticancer Drug Carriers. *Mol. Pharm.* **2005**, *2*, 475–480.
11. Murakami, T.; Fan, J.; Yudasaka, M.; Iijima, S.; Shiba, K. Solubilization of Single-Wall Carbon Nanohorns Using a PEG-Doxorubicin Conjugate. *Mol. Pharm.* **2006**, *3*, 407–414.
12. Matsumura, S.; Ajima, K.; Yudasaka, M.; Iijima, S.; Shiba, K. Dispersion of Cisplatin-Loaded Carbon Nanohorns with a Conjugate Comprised of an Artificial Peptide Aptamer and Polyethylene Glycol. *Mol. Pharm.* **2007**, *4*, 723–729.
13. Chen, R.; Zhang, Y.; Wang, D.; Dai, H. Noncovalent Sidewall Functionalization of Single-Walled Carbon Nanotubes for Protein Immobilization. *J. Am. Chem. Soc.* **2001**, *123*, 3838–3839.
14. Huang, W.; Taylor, S.; Fu, K.; Lin, Y.; Zhang, D.; Hanks, T. W.; Rao, A. M.; Sun, Y.-P. Attaching Proteins to Carbon Nanotubes *via* Diimide-Activated Amidation. *Nano Lett.* **2002**, *2*, 311–314.

15. Georgakilas, V.; Kordatos, K.; Prato, M.; Guldi, D. M.; Holzinger, M.; Hirsch, A. Organic Functionalization of Carbon Nanotubes. *J. Am. Chem. Soc.* **2002**, *124*, 760–761.
16. Yuge, R.; Yudasaka, M.; Miyawaki, J.; Kubo, Y.; Ichihashi, T.; Imai, H.; Nakamura, E.; Isobe, H.; Yorimitsu, H.; Iijima, S. Plugging and Unplugging Holes of Single-Wall Carbon Nanohorns. *J. Phys. Chem. C* **2007**, *111*, 7348–7351.
17. Becker, M. L.; Fagan, J. F.; Gallant, N. D.; Bauer, B. J.; Bajpai, V.; Hobbie, E. K.; Lacerda, S. H.; Migler, K. B.; Jakupciak, J. P. Length-Dependent Uptake of DNA-Wrapped Single-Walled Carbon Nanotubes. *Adv. Mater.* **2007**, *19*, 939.
18. Iijima, S. Helical Microtubules of Graphitic Carbon. *Nature* **1991**, *354*, 56–58.
19. Tohji, J.; Goto, T.; Tkahashi, H.; Shinosa, Y.; Shimizu, N.; Jeryadevan, B.; Matsuoka, I.; Saito, Y.; Kasuya, A.; Ohsuna, T.; et al. Purifying Single-Walled Nanotubes. *Nature* **1996**, *383*, 679.
20. Miyawaki, J.; Yudasaka, M.; Azami, T.; Kubo, Y.; Iijima, S. Toxicity of Single-Walled Carbon Nanohorns. *ACS Nano* **2008**, *2*, 213–226.
21. Iijima, S.; Yudasaka, M.; Yamada, R.; Bandow, S.; Suenaga, K.; Kokai, F.; Takahashi, K. Nano-Aggregates of Single-Walled Graphitic Carbon Nanohorns. *Chem. Phys. Lett.* **1999**, *309*, 165–170.
22. Azami, T.; Kasuya, D.; Yuge, R.; Yudasaka, M.; Iijima, S.; Yoshitake, T.; Kubo, Y. Large-Scale Production of Single-Wall Carbon Nanohorns with High Purity. *J. Phys. Chem. C* **2008**, *112*, 1330–1334.
23. Murakami, T.; Sawada, H.; Tamura, G.; Yudasaka, M.; Iijima, S.; Tsuchida, K. Water-Dispersed Single-Wall Carbon Nanohorns as Drug Carriers for Local Cancer Chemotherapy. *Nanomedicine* **2008**, *3*, 453–63.
24. Pinto, A. L.; Lippard, S. J. Binding of the Antitumor Drug *cis*-Diamminedichloroplatinum(II) (Cisplatin) to DNA. *Biochim. Biophys. Acta* **1985**, *780*, 167–180.
25. Zwelling, L. A.; Kohn, K. W. Mechanism of Action of *cis*-Dichlorodiammineplatinum(II). *Cancer Treatment Rep.* **1979**, *63*, 9–10.
26. Raudaschl, G.; Lippert, B.; Hoeschele, J. D.; Howard-lock, H. E.; Lock, C. J. L.; Pilon, P. Adduct Formation of *cis*-$(NH_3)_2PtCl_2(CH_3)_2NCHO$. Application for the Purification of the Antitumor Agent Cisplatin. *Inorg. Chim. Acta* **1985**, *106*, 141–149.
27. Fan, J.; Yudasaka, M.; Kasuya, D.; Azami, T.; Yuge, R.; Imai, H.; Kubo, Y.; Iijima, S. Micrometer-Sized Graphitic Balls Produced Together with Single-Wall Carbon Nanohorns. *J. Phys. Chem. B* **2005**, *109*, 10756–10759.
28. Fan, J.; Yudasaka, M.; Miyawaki, J.; Ajima, K.; Murata, K.; Iijima, S. Control of Hole Opening in Single-Wall Carbon Nanotubes and Single-Wall Carbon Nanohorns Using Oxygen. *J. Phys. Chem. B* **2006**, *110*, 1587–1591.